Eur Phys J C **33**, s01, s442–s444 (2004)
Digital Object Identifier (DOI) 10.1140/epjcd/s2004-03-1657-0

EPJ C direct
electronic only

Studies of two-photon collisions at LEP2

Imre Pál[a], on behalf of the LEP wide Working Group on Two Photon Physics

Department of Physics, Purdue University, 525. Northwestern Avenue, West Lafayette, Indiana, 47907-2036 USA

Received: 5 November 2003 / Accepted: 7 January 2004 /
Published Online: 13 February 2004 –

Abstract. A review of the recent experimental results on two-photon physics at LEP2 is presented. Differential cross-sections are measured for double-tagged hadronic $\gamma\gamma$ events by the ALEPH and OPAL collaborations. Single particle inclusive differential cross-sections are measured by the L3 experiment at center-of-mass energies between 189 GeV and 202 GeV. For the first time at LEP the production of prompt photons is studied in the collision of quasi-real photons using data taken by the OPAL experiment at LEP2 energies.

1 Introduction

Photons can interact with hadrons either *directly* by coupling to the electric charge of quarks or according to the *Vector Dominance Model* (VDM) where the photon couples to a vector meson carrying the same quantum numbers as the photon. If a quark (or a QCD evolved quark or gluon) coupling to the photon in either of the above ways participates in a hard scattering process it is said to originate from a *resolved* photon. These different photon-hadron interactions are illustrated in Fig. 1.

The classical way to investigate the structure of the photon at e^+e^- colliders is the measurement of the process

$$e^+e^- \to e^+e^-\gamma\gamma \to e^+e^-X,$$

where the photons can be quasi-real or virtual and X denotes the hadronic final state. If both the electron and positron are observed (*double − tagged*) the dynamics of highly virtual photon collisions is probed. If only one electron is observed (*single − tagged*) the process can be described as deep-inelastic electron scattering off a quasi-real photon. These events have been studied to measure both leptonic and hadronic photon structure functions. In the case where none of the electrons is observed (*untagged*), the structure of the quasi-real photon is studied in terms of total cross-sections, jet production and heavy quark production.

2 Hadronic final states in $\gamma\gamma$ collisions

As shown in Fig. 1., the process of $\gamma\gamma \to$ *hadrons* has contributions from a "soft" VDM interaction, a point like two photon reaction and a "hard" resolved component (single and double). The $\gamma\gamma \to q\bar{q}$ process is exactly calculable in QED, whereas the resolved processes are sensitive to the density of quarks and gluons in the photon.

[a] *Present address:* CERN, Division EP, CH-1211 Geneva 23

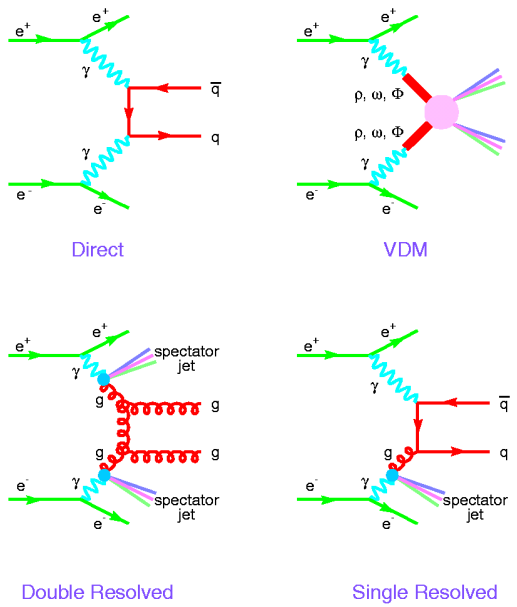

Fig. 1. Hadronic final states in two-photon collisions

The VDM process dominates in the "soft" interaction region, where hadrons are produced with a low transverse momentum p_T. Hadrons with high p_T are produced by the QED process $\gamma\gamma \to q\bar{q}$ or by resolved processes.

3 Two-photon processes

3.1 Double-tagged $\gamma\gamma$ events

Double-tagged hadronic events in two photon collisions are studied at LEP by the ALEPH [1], L3 [2] and OPAL [3] collaborations. The $\gamma^*\gamma^*$ interaction can be seen as the interaction of two $q\bar{q}$ pairs scattering off each other via

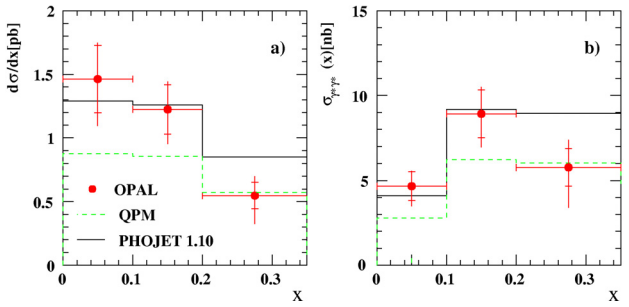

Fig. 2. Cross-sections for *a*, the process $e^+e^- \to e^+e^-hadrons$ in the region $E_{1,2} > 0.4\ E_{beam}$, $34 < \theta_{1,2} < 55$ mrad and $W > 5$ GeV, and for *b*, the process $\gamma^*\gamma^* \to hadrons$, as function of x for $\langle Q^2 \rangle = 17.9$ GeV^2

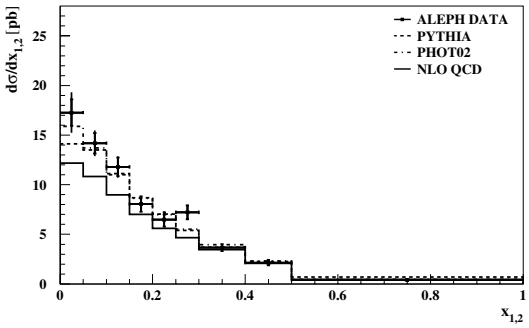

Fig. 3. Differential cross-section as a function of the deep inelastic scattering variable x in the phase space defined by the electron energies $E_{1,2} > 0.3\ E_{beam}$, the polar angles of the electrons $35 < \theta_{1,2} < 155$ mrad and the mass of the hadronic system $W_{\gamma\gamma} > 3$ GeV

multiple gluon exchange. For processes with large photon 4-momentum transfer squared and $Q_1^2 \simeq Q_2^2$, the calculation can be performed without phenomenological inputs as non-perturbative QCD contributions are expected to vanish. An effective two-photon cross-section, $\sigma_{\gamma^*\gamma^*}$, is extracted from the $e^+e^- \to e^+e^-hadrons$ cross-section, σ_{ee}, by using the QED calculable transverse photon luminosity function; $L_{TT} = \sigma_{ee}/\sigma_{\gamma^*\gamma^*}$.

Differential cross-sections are measured as function of several kinematical variables ($x, Q^2, W_{\gamma\gamma}, Y$,etc.). The majority of measured distributions are well described in shape by Monte Carlo models but require adjustments in normalization to match the data. In Fig. 2 and Fig. 3. cross-sections as funtion of the Björken variable x are shown from the OPAL and ALEPH experiment, respectively. The NLO QCD predictions also give resonable description lying slightly below the data as shown in Fig. 3.

The cross-section measurement for scattering of two virtual photons is considered as "golden" process to test the BFKL dynamics. To compare data to BFKL calculations the variable $Y = ln(s/s_0) \simeq ln(W^2_{\gamma^*\gamma^*}/\sqrt{Q_1^2 Q_2^2})$ is defined. As shown in Fig. 4. the LO BFKL calculation is barely in agreement with the data for any value of the Regge scale parameter. Calculations including dominant higher order corrections and the NLO BFKL calculations predict smaller effects in the LEP range and are found to

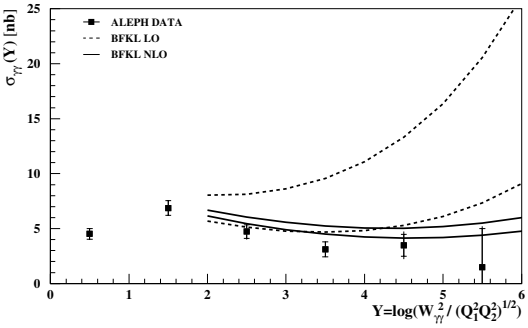

Fig. 4. The $\sigma_{\gamma\gamma}$ cross-section as a function of Y in comparison with LO BFKL and NLO BFKL, the range giving the uncertainty estimated from the variation of the Regge scale parameter from Q^2 to 10 Q^2 and from Q^2 to 4 Q^2, respectively

be consistent with the measured cross-sections. The limited statistics and available Y range of the data prevent establishing or ruling out the onset of BFKL dynamics in this reaction.

3.2 Inclusive single particle production

Inclusive charged hadron [7] and inclusive π^0 and K_S^0 [8] production in two-photon collisions were studied by the L3 collaboration at LEP2 energies using data corresponding to 414 pb^{-1} of integrated luminosity. Inclusive π^0 production is measured via the decay $\pi^0 \to \gamma\gamma$ associated to two electromagnetic clusters while inclusive K_S^0 production is measured using the decay $K_S^0 \to \pi^+\pi^-$. Assuming the fragmentation functions implemented in JETSET are correct, the $\pi^\pm$ and the $K^\pm$ inclusive cross-sections are extracted from the charged hadron cross-section. Good agreement is found between the extracted $\pi^\pm$, $K^\pm$ cross section and the measured π^0, K_S^0 ones. Differential cross-sections as a function of the transverse momentum p_T and of the pseudorapidity $|\eta|$ are calculated for $W_{\gamma\gamma} \geq 5$ GeV and a photon virtuality $Q^2 \leq 8$ GeV^2. Results are shown in Fig. 5. The data are compared to NLO QCD predictions. The behavior of $d\sigma/dp_T$ in the low-p_T range is described by an exponential which is characteristic of hadrons produced by soft interactions. At higher p$_T$ the exponential behaviour breaks down due to the direct $\gamma\gamma \to q\bar{q}$ process and resolved photon interactions. The agreement of the NLO QCD prediction with the data is satisfactory in the K_S^0 case (only low p_T region is measured) but, as shown in Fig. 5.a, it is poor for the π^0 and also for the charged hadron cases in the high-p_T range for any choice of scale. Figure 5.b shows that the shape of the $d\sigma/d|\eta|$ differential cross-section is reproduced by NLO QCD prediction.

3.3 Isolated prompt photon production

In leading order, prompt photons are restricted to resolved processes, i.e. to processes in which at least one of the incoming photons has fluctuated into hadrons. Therefore,

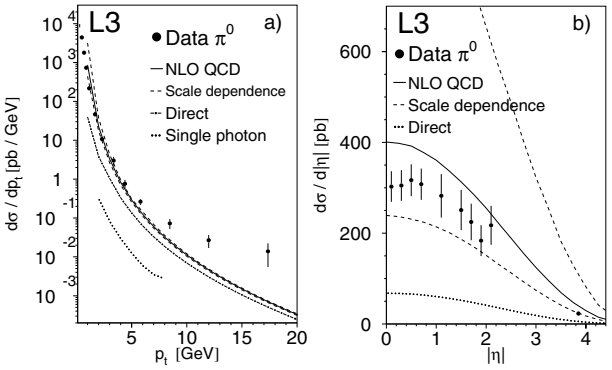

Fig. 5. Inclusive differential cross-sections $d\sigma/dp_T$ and $d\sigma/d|\eta|$ compared to NLO QCD predictions for π^0 production for a, $|\eta| < 0.5$ b, $p_T > 1$GeV. The NLO calculations are given for the QCD scale equal to p_T (*solid line*) and for the scales 0.5 p_T (*upper dashed line*) and 2 p_T (*lower dashed line*). The contribution of the direct QED process is also indicated

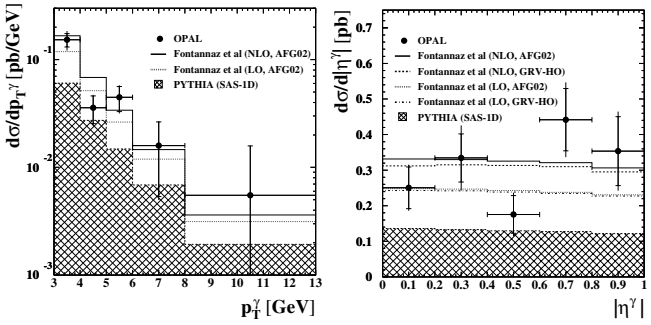

Fig. 6. Differential cross-sections $d\sigma/dp_T$ and $d\sigma/d|\eta|$ for inclusive prompt photon production in the kinematic range $|\eta| < 1$ and $p_T > 3.0$ GeV

prompt photons can be used to investigate the hadronic substructure of the photon. The event signatures are usually less subject to hadronization corrections than are dijet or hadronic signatures which are also used to extract the photonic substructure. However, the cross-section for prompt photon production is typically smaller by a factor of $1/\alpha_{EM}$ than the dijet cross-section.

The data used in the analysis were taken by the OPAL [6] detector at center-of-mass energies $\sqrt{s} = 183$-209 GeV and correspond to an integrated luminosity of about 649 pb^{-1}. Since over this energy range the variation of the cross-section for prompt photon production is expected to be less than the statistical error of the data, all energies are analysed together.

The event selection is set up so that only anti-tagged photon-photon collision events are kept, i.e. events with a scattered $e^{\pm}$ detected are rejected. Isolated photon candidates are then searched for in the electromagnetic calorimeter. A photon signal can originate from a prompt photon but also from π^0 or η mesons decaying into two photons as well as annihilation of antineutrons, $\bar{n}$, in the detector material. A cluster shape analysis is used to remove background events. In order to reject photons from particle decays or fragmentation processes, the isolation criterion suggested by Frixione [9] was applied. Events with more than one candidate photon are rejected. After applying all cuts the total cross-section is measured to be $\sigma = 0.32 \pm 0.04(stat) \pm 0.04(sys)$ pb.

The differential cross-sections in p_T and $|\eta|$ have been studied and compared to predictions of an NLO QCD calculation by Fontannaz *et al.* [10] and of the PYTHIA Monte Carlo program using the SaS-1d photon parton density distributions.

As shown in Fig. 6. in both cases PYTHIA reproduces the shape of the distributions well but underestimates the cross-sections, whereas the NLO calculation describes well the shape and normalization of the data.

4 Conclusion

In case of double-tagged hadronic events a good agreement with Monte Carlo simulations and NLO BFKL calculations was found. The production of isolated prompt photons is described well by NLO QCD calculation for 3 GeV $< p_T^\gamma <$ 12 GeV. For inclusive single hadron production good agreement is found for $p_T < 4$ GeV when the NLO QCD calculation is compared to data but a large excess is observed in the range of 10 GeV $< p_T <$ 20 GeV.

References

1. A. Heister, *et al.* - ALEPH Collaboration: hep-ex/0305107 (2003)
2. P. Achard, *et al.* - L3 Collaboration: Phys. Lett. B **531**, 39-51 (2002)
3. G. Abbiendi, *et al.* - OPAL Collaboration: Eur. Phys. J. C **24**, 17-31 (2002)
4. M. Cacciari, V. Del Duca, S. Frixione, and Z. Trócsányi: JHEP **02**, 29 (2001)
5. S.J. Brodsky, V.S. Fadin, V.T. Kim, L.N. Lipatov, and G.B. Pivovaro: JETP Lett., **Vol.76, No. 5.**, 249-252 (2002)
6. G. Abbiendi, *et al.* - OPAL Collaboration: CERN-EP/2003-023
7. P. Achard, *et al.* - L3 Collaboration: Phys. Lett. B **554**, 105-114 (2003)
8. P. Achard, *et al.* - L3 Collaboration: Phys. Lett. B **524**, 44-54 (2002)
9. S. Frixione: Phys. Lett. B **429**, 369 (1998)
10. M. Fontannaz, J.P. Guillet, and G. Heinrich: Eur. Phys. J. C **23**, 503 (2002)